

Acoustic characterisation of two parallel supersonic jets

Piantanida, Selene¹
Université de Poitiers
15, rue de l'Hotel Dieu, 86000, Poitiers

Berterretche, Patrick²
Université de Poitiers
15, rue de l'Hotel Dieu, 86000, Poitiers

ABSTRACT

In the context of the development of the Ariane 6 launch vehicle, the acoustic characteristics of two parallel, supersonic, heated jets ($Mach=3$, $T=1600K$) have been investigated. Acoustic measurements were made by means of four polar arrays of microphones in the far-field, as well as by a circular antenna surrounding the mock-up body, to investigate the upstream sound emission. A simplified configuration, where one of the two jets were obstructed, has also been studied for comparison, in order to analyse the jets interaction effects. A series of PIV measurements has been conducted with the aim of understanding the mean flow modification induced by the double configuration. Results show no considerable interaction between the hydrodynamic fields of the parallel jets, while a significant change occurs in the sound field. An asymmetric behaviour is observed, depending on the azimuthal observation angle: in the plane containing the axes of the two jets, the increase in the measured sound intensity (wrt the simple jet configuration) is half of the one observed in the perpendicular plane, indicating an acoustic shielding mechanism between the jets.

Keywords: Twin-jets, Jet noise, PIV

I-INCE Classification of Subject Number: 74

(see <http://i-ince.org/files/data/classification.pdf>)

1. CONTEXT

The new generation of European space launchers is represented by the new Ariane 6 model, developed by the European Space Agency, that will substitute the current Ariane 5 version in 2020. The first stage propulsion system will be composed of a central cryogenic

¹selene.piantanida@univ-poitiers.fr

²patrick.berterretche@univ-poitiers.fr

stage (Vulcain), powered by liquid oxygen and hydrogen, surrounded by 2 or 4 solid rocket boosters providing additional thrust and main acoustic sources at the launching phase. The acoustic qualification of the launch site is however based on an equivalent acoustic power, obtained as a simple superposition of the sources of each booster, the mutual interaction between the jets being neglected. This study, in the context of the future development of the Ariane 6 launcher, aims at giving a set of reference experimental data about the acoustic environment in the immediate surroundings of the launch area.

2. INTRODUCTION

Twin-jets configurations has been traditionally used to suppress turbojet engine noise and were firsts proposed by Greatrex and Brown [1]. A number of studies has been carried out since then to explore and understand the phenomenology responsible for the acoustic modifications induced by the coupling of the two jets.

The aerodynamic structure of two high-speed jets has been studied by Elangovan *et al* [2], for parallel and non parallel flows. The nozzle spacing was also varied as well as the operating Mach number. The authors divided the jets development in three different regions: a first region where the jet are independent, a mixing region starting where first the mixing layer touch and a combined region where the two jets are completely merged. Through the study of the center-line velocities, they observed that the merging distance and the length of the mixing zone strongly depend on the nozzle geometrical parameters, namely the inter-nozzle spacing and the angle α defining the jets inclination towards each other. These quantities are in turn fundamental in the definition of the acoustic properties of the twin-jets. The main effect observed for coupled jets is that of acoustic shielding, observed by a number of studies [3–7]. It is caused by the refraction, diffraction and reflection mechanisms of the acoustic waves and results in a lower noise radiation in the plane containing the jet axis with respect to the perpendicular direction. The modelling work proposed in the cited works remains limited to a narrow set of flow and geometrical parameters, which do not include the high temperature and velocity considered here. The interest of this work is thus to characterize the velocity field for two supersonic, hot jets (in conditions that are representative of the Ariane launching) and to compare the acoustic measurements to the theoretical predictions proposed in the literature.

3. EXPERIMENTAL CONFIGURATION

The experiments took place at the MARTEL (Moyen Aéroacoustique de Recherche et Technologie sur l'Environnement des Lanceurs) facility in the Centre d'Études Aérodynamiques et Thermiques (CEAT) in Poitiers, France. Born from the cooperation of the Université de Poitiers with the Centre National d'Études Spatiales (CNES, national organisation for space research), its main purpose is to study the noise generation of very fast and very hot jets. The configuration used, called 'booster configuration', is used to generate an axisymmetric, supersonic jet. The flow is created by a pressurised air supply (of pressure $P = 30 \text{ bar}$), issuing from a convergent-divergent, conical nozzle of throat and exit diameter of respectively $d_t = 24.5 \text{ mm}$ and $D = 60 \text{ mm}$. It is then heated up to 1600 K by means of an air-hydrogen combustion taking place before the nozzle. The nozzle geometry and the upstream functioning conditions (supply pressure and temperature) generate a slightly over-expanded jet. The jet is in vertical position, directed towards the floor, with the nozzle exit at a height of 3 meters, corresponding to

50 D . A special bi-nozzle geometry has been designed to meet the requirements of this study: after the combustion chamber, as visible in picture 1, the flow is separated in two ducts to generate the two identical parallel jets. The interaxial distance is fixed and equal to $d_j = 168 \text{ mm} = 2.8 D$.

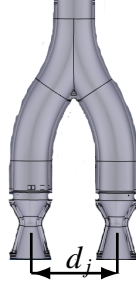


Figure 1: Scheme of the double nozzle geometry used to produce the parallel jets.

In order to compare the twin jets results with a single jet configuration, a series of measurements have been performed with one of the two jets blocked, in order to minimize the installations effects on the data analysis.

Two separate measurement campaigns have been carried out: during the first one, the mean velocity field has been investigated by means of a 2D, 2-components PIV (Particle Image Velocimetry) system, covering the whole development of the jets. Successively, a system of 5 microphone antennae has been installed around the twin-jets body as well as in the jet acoustic field to measure the emitted sound field. More details about the measurement systems are given in the next sections.

3.1 PIV instrumentation

The main velocity field has been measured in a longitudinal plane containing the axis of the two jets. Two cameras LaVision Imager LX 16M and an EverGreen, 200mJ laser have been mounted in the experimental hall, on special supports that guaranteed a precise positioning in the vertical direction. An overview of the installation is shown in figure 2a, as well as a zoom on the twin-jets nozzle exit (2b).

The two cameras have been simultaneously used, one on the top of the other as showed in figure 3a, each covering 5 jet diameters in the downstream direction. The objective being to understand the development and the interaction between the two jets till a complete mixing, a series of 4 successive measurements have been made as to map the flow field up to $42 D$ (and $25 D$ for the simple jet configuration). A scheme of the camera views for each set of measurements is shown in figure 3b, where J1 and J2 represent the twin jets and the numbered squares the camera positions. For each configuration, a partial superposition of the fields of view assures the image continuity. Due to the spreading of the jet as the longitudinal coordinate is increased, the camera field of view has also been enlarged, from $L = 8 D$ for the position 1 to 3, to $L = 11 D$ for the other four. The position and size of each visualisation window in the x direction is summarized in table 1, where H and L are respectively the window height and width, and all the quantities are expressed in terms of the nozzle exit diameter D .

The flow seeding is composed of micro-metric silica (SiO_2) particles, which are adapted, in terms of dimensions and thermal characteristics, to the velocity and temperature conditions considered. Two separate seeding systems have been used: a first one assures the seeding of the twin-jets flow field, injecting the particles upstream the

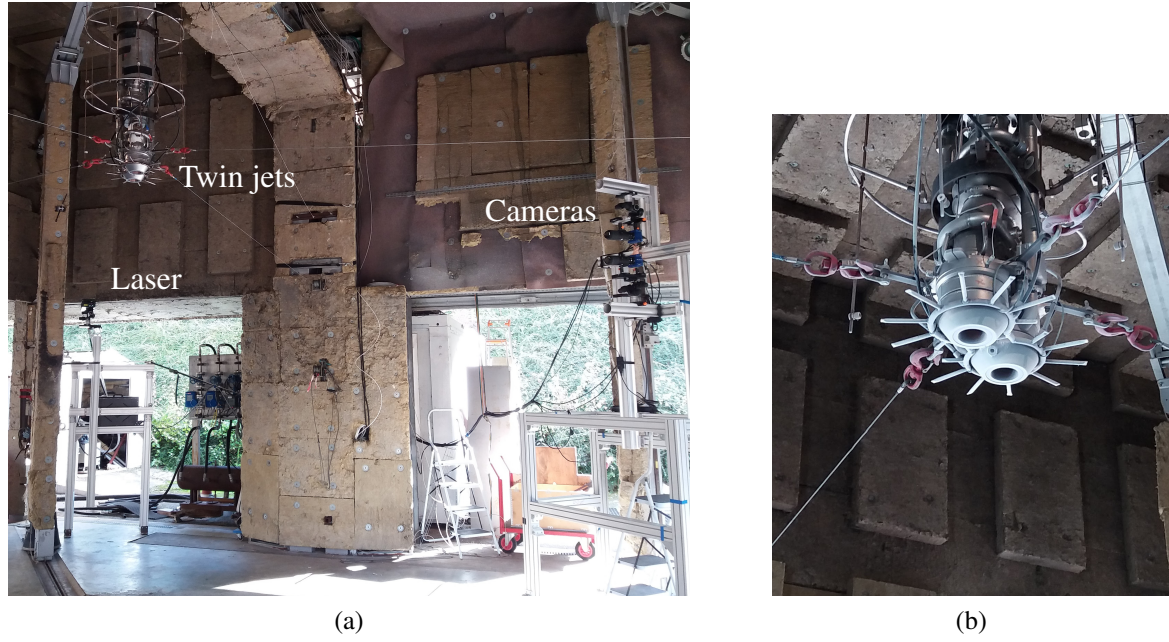


Figure 2: a): Experimental hall with the twin-jets system and the PIV instrumentation. b): Detail of the twin-jets nozzle exit where the external seeding ring is visible.

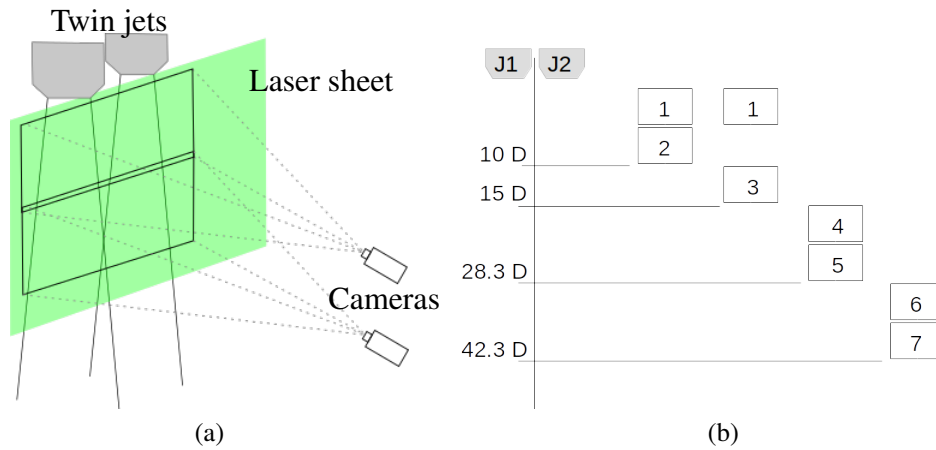


Figure 3: Configuration of the camera positions.

combustion chamber, while a secondary one is used to spread particles at the exterior of the nozzles, allowing the visualisation of the mixing layer. This is done by a special perforated ring positioned at the nozzle exit (the sun-like structure visible in figure 2b) and fed by a pressurized air circuit.

3.2 Acoustic measurements

The acoustic field has been investigated by means of a total number of 26 microphones, distributed on 5 antennae.

An azimuthal antenna is placed slightly upstream of the nozzle exit, with respect to the flow direction (figure 4). It has an oval shape, to enclose the double jet geometry, and is equipped of 6 microphones to allow the evaluation of the jets symmetry. Two microphones are placed in a plane containing the axis of both jets, and the others in the

Table 1: Camera window for each position.

Camera position	1	2	3	4	5	6	7
field of view dimensions, H/L (D)	5.3 / 8	5.3 / 8	5.3 / 8	7.4 / 11	7.4 / 11	7.9 / 11	7.9 / 11
window covering in x direction (D)	[-0.08,5.25]	[5,10.3]	[9.92,15.2]	[14.6,22]	[21.35,28.7]	[28,35.9]	[34.6,42.4]

two planes perpendicular to this one passing through the two jets axis. The radial distance of the microphones from the jet center is $r_m = 31 \text{ cm} = 5.2 D$.

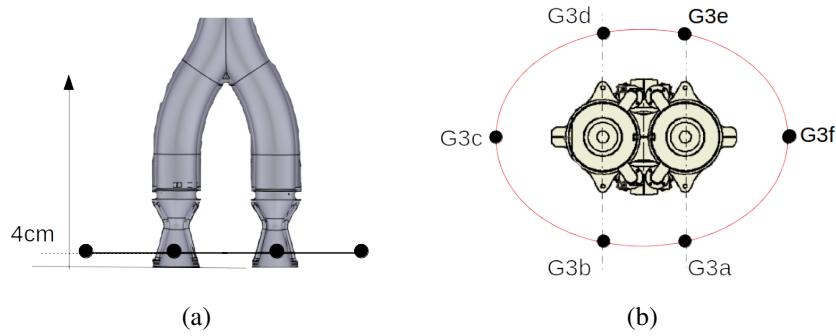


Figure 4: Microphones position on the antenna at the nozzle exit.

In addition, four polar antennae are used to observe the twin-jets directivity in the far field (figure 5). They are placed at a distance of 150 cm from the symmetry point of the nozzle plane, corresponding to $25 D$, and cover a polar arc from $\theta = 30^\circ$ to $\theta = 110^\circ$, the reference being the downstream direction. They are equipped with 7 or 3 microphones, as shown in the picture, and are placed in the two symmetry planes of the double-jet configuration, identified by means of the azimuthal angle ϕ , where the angle $\phi = 0^\circ$ is the plane containing the axis of the two jets.

4. RESULTS

4.1 Mean velocity field

The seven velocity fields measured for the different camera positions have been assembled to form a single, complete representation of the jets, for the two configurations studied. In figure 6, the mean axial velocity field of the two configurations considered is showed, where the spacial coordinates are normalised by the nozzle exit diameter D , for the pressure and temperature conditions $P = 30 \text{ bar}$ and $T = 1600 \text{ K}$. The calculated fields have been normalised by the axial exit velocity, V_{x_e} , defined as the maximum velocity at the axial coordinate $x/D = 0.13$. This is equal to $V_{x_e} = 1590 \text{ m/s}$ pour la configuration jet simple, while a minor dissymmetry, probably due to a slight geometric dissymmetry of the mock-up, has been observed for the double jet, with $V_{x_e_J1} = 1675 \text{ m/s}$ and $V_{x_e_J2} = 1645 \text{ m/s}$ ($J1$ and $J2$ being the two jets). The relative difference between the two configurations, which remains under 5%, is linked to a variation in the upstream conditions of temperature and pressure. A greater variation of those quantities, with respect to the acoustic campaign, has been observed during the PIV

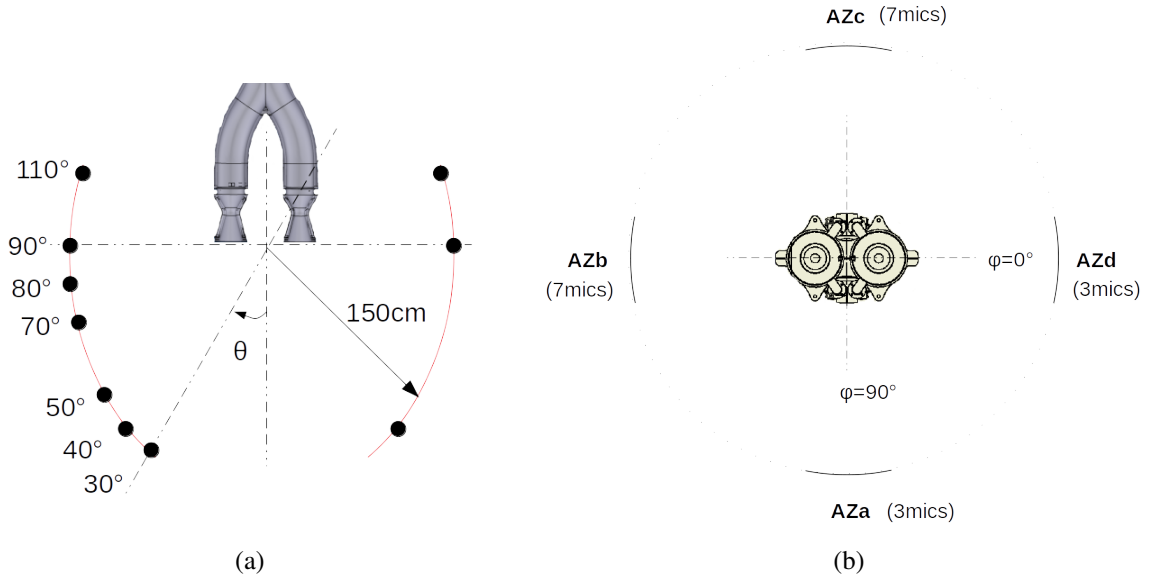


Figure 5: Polar antennae configuration and microphones position in the far field.

measurements, due firstly to the SiO₂ particles injection, which causes a temperature drop of about 100° for the double jet configuration, and to the long duration of the measurements (about 4 minutes), which leads to an inertial derivation of the regulation parameters. This results to an overall higher dispersion of the generating conditions upstream of the nozzles.

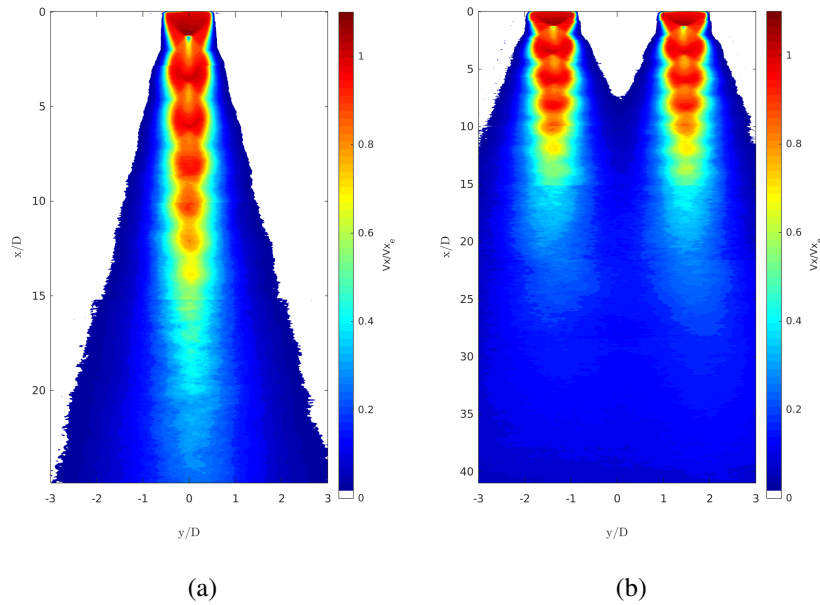


Figure 6: Total mean axial velocity field for the simple and twin-jets configurations.

4.1.1 Simple jet vs twin-jets comparison

The jet presents a classical shock cell structure (figure 7a), developing on approximately 15 diameters, with seven visible shock cells. The flow, transitioning from the in-nozzle conditions, is then compressed through a shock wave at about $x/D = 1.3$. Downstream the shock, in the developed zone, a series of compression and expansion waves allows the jet to fully adapt to the ambient pressure. A good symmetry of the jets can be observed in figure 7b, where the measured radial component of the velocity field is shown.

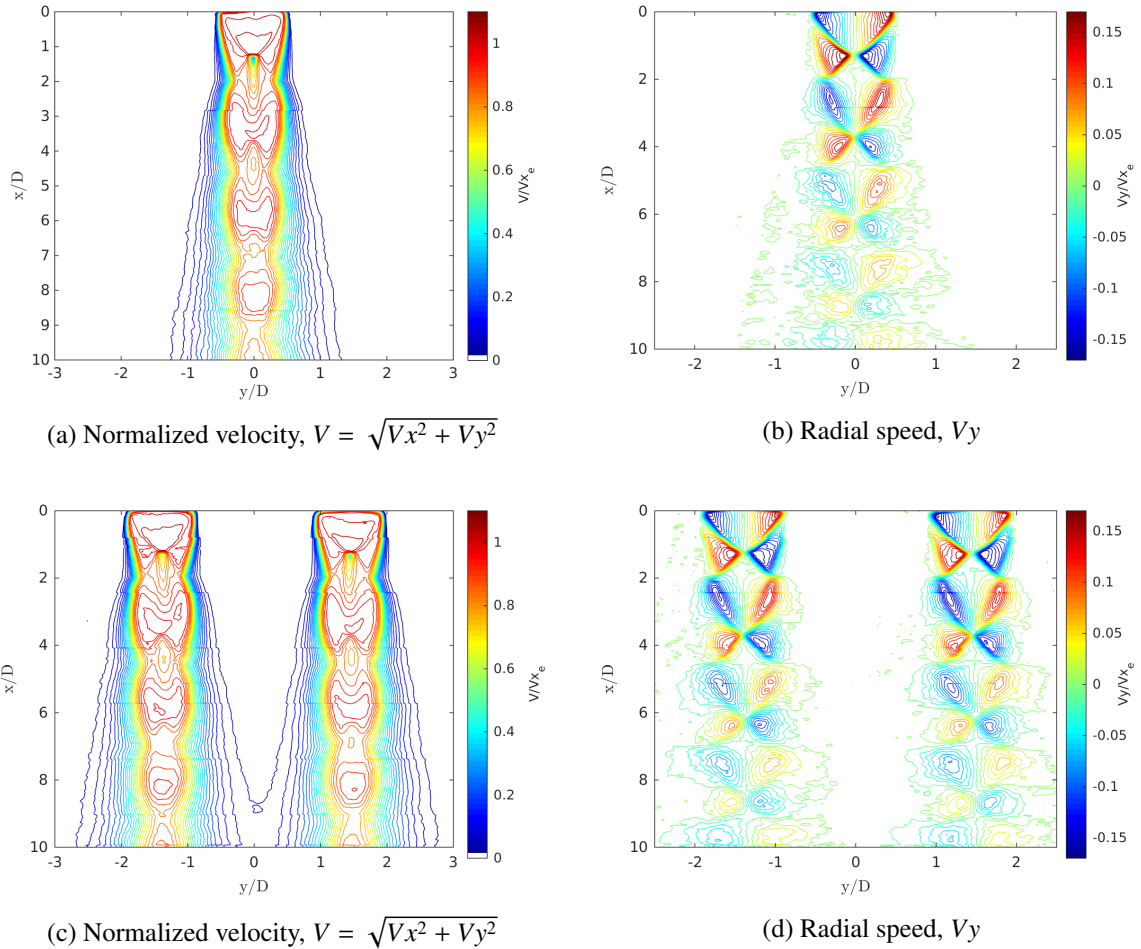


Figure 7: Velocity contours in the plane containing the jet axis for the two configurations studied. Top row: simple jet; bottom row: twin-jets.

As visible in figures 7c and 7d, the aerodynamic structure of the twin-jets configuration is very close to that of the simple jet. Three different zones can be identified: from the nozzle exit till around $x/D = 10$, the two jets behave as independent from each other. The spreading angle, the shock position, the amplitude and length of the shock cells (see also figure 8a) are identical to those of the simple jet. A small inflection of the jets seems to happen, manifest in a slight dissymmetry of the velocity contours towards the inter-axe of the two jets in figure 7d, but it is not sufficiently significant to conclude about an interaction occurring between the two jets. From about $x/D = 10$, the two aerodynamic fields begin to interact and the inner mixing layers to merge. This is shown in figure 8b, where radial profiles of the axial velocity are plotted for different axial coordinates:

starting at that position the axial velocity at the symmetry plan is different from 0 and increases farther downstream. In the third zone, extending from approximately $x/D = 30$ to the end of the measuring domain, the two jets are completely merged and the velocity profile is equivalent to the one of a single jet.

A comparison between the mean, axial velocity profile, measured on the jet axis, of the simple jet and the twin-jets is represented in figure 8a. For both configurations the velocity jump induced by the shock is really well captured, with a measured relative amplitude discontinuity of $\Delta V = 0.8 V_x/V_{x_e}$. As already said, the velocity profiles for the twin-jets configuration are perfectly superposed to the simple jet, meaning that no mutual interaction occurs between the two flows. Starting from about $x/D = 10$, a difference begins to appear as the mixing layers merge, but further analysis is necessary to fully understand the effects of this interaction.

From the experimental measurements, it is possible to calculate the length of the shock cells, characteristic dimension of the jet's aerodynamic structure and key parameter for the acoustic radiation. Based on the average length of the first four cells, measured as the distance between two successive maximum of the axial velocity, the experimental cell length is $L_c = 2.3 D = 140 \text{ mm}$. A theoretical value for this quantity can be estimated by means of the formula proposed by Tam and Tanna [8]: $L_c = 1.03(M_j^2 - 1)^{0.5} D_j$. For the temperature and pressure conditions considered in this campaign, the theoretical cells length differs from the experimental one by 15%.

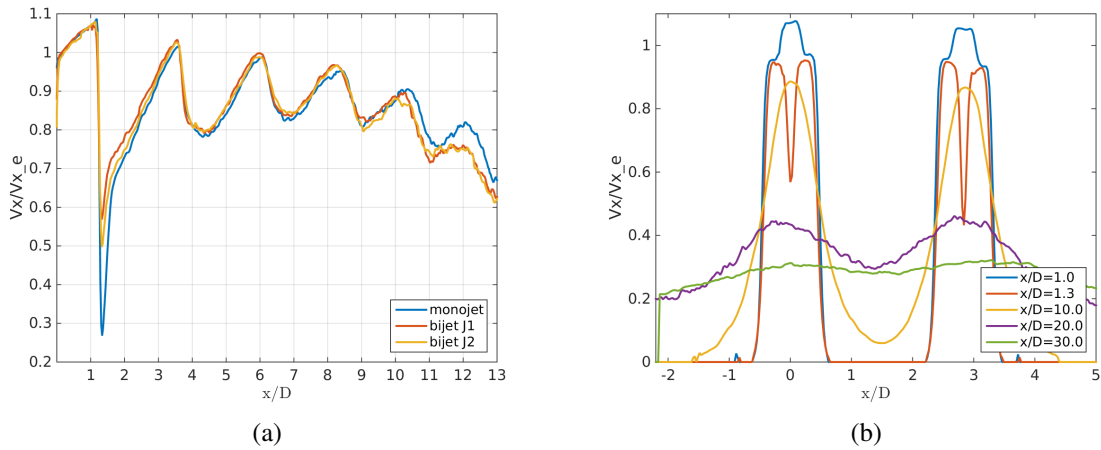


Figure 8: a): Comparison between the mean axial velocity profiles, measured by PIV on the jet axis, for a single jet and a twin-jets configuration. b): Mean axial velocity profiles in radial direction for the twin-jets configuration.

4.2 Acoustic field

As described in section 2, the noise radiation of a supersonic, imperfectly expanded jet is generally composed of three principal sources: screech, mixing noise and shock-associated noise. The three mechanisms have a different weight depending on the jet conditions in terms of velocity and temperature. At a temperature of 1600 K, as considered here, the screech component disappears and the noise spectrum is dominated by the mixing noise, with a marked peak characteristic of the shock-cell noise, as the observer is at polar angles greater than $\sim 70^\circ$.

In figure 9, the sound spectra (SPL) and the overall sound pressure levels (OASPL) measured by the polar antennae AZ_c are shown for the single jet configuration as function of the observation polar angle θ . The SPL is defined as $SPL = 10 \log_{10}(PSD/p_{ref}^2)$, where PSD is the power spectral density of the pressure fluctuations and $p_{ref} = 2 \cdot 10^{-5} Pa$, and the Strouhal number St represents a non-dimensional frequency: $St = fD_j/U_j$. The OASPL has been calculated as integration of the SPL between $0.04 \leq St \leq 2.3$ ($700Hz \leq f \leq 40 kHz$). The overall noise emission decays as the polar angle is increased, but the spectral distribution of the sources responsible for this behaviour is different for each polar angle. At angles near the jet axis ($\leq 50^\circ$), the spectra presents a broad-band peak, characteristic of the mixing noise, whose central frequency depends on the angle itself. As θ is moved towards the direction normal to the jet axis, the shock-associated noise dominates over the mixing noise, with a narrower peak, whose frequency decreases at higher angles.

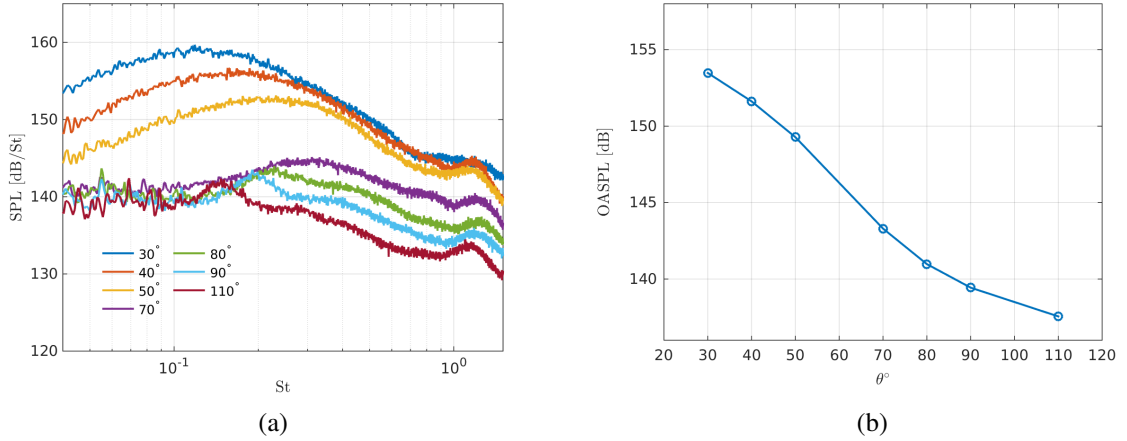


Figure 9: Polar SPL and OASPL calculated in the acoustic field for the simple jet configuration.

The acoustic radiation associated with the twin-jets presents a more complex phenomenology. Despite a very limited aerodynamic interaction observed between the jets, a highly asymmetric behaviour is measured for both the polar antennae and the near-nozzle microphones. In figure 10, the SPL and OASPL for the six microphones on the oval antenna in the nozzle-exit plan are shown. The two microphones positioned in the plan containing the axis of both jets ($\phi = 0$) measure lower overall noise level (of about 1.5dB) with respect to the sensors in the perpendicular positions. This reduction affects the entire spectrum, starting from the peak frequency. This reduction, given the positioning of the two microphones, indicates a possible acoustic masking effect occurring between the two jets.

The analysis of the spectra in the acoustic field also shows a behaviour that depends on the azimuthal angle of observation. In figures 11a and 11b, a comparison between the spectra measured at perpendicular directions is presented. The peak shape, intensities and frequencies strongly depend on the azimuthal angle ϕ . For the lowest polar angles, the peak associated with the mixing noise appears to be stronger and centred at a higher frequency when the observer is in the plane $\phi = 90$. At the highest polar angles, on the contrary, the peak corresponding to the shock-associated noise appears to be weaker, which suggest that a different effect is generated by the jets interaction on the various

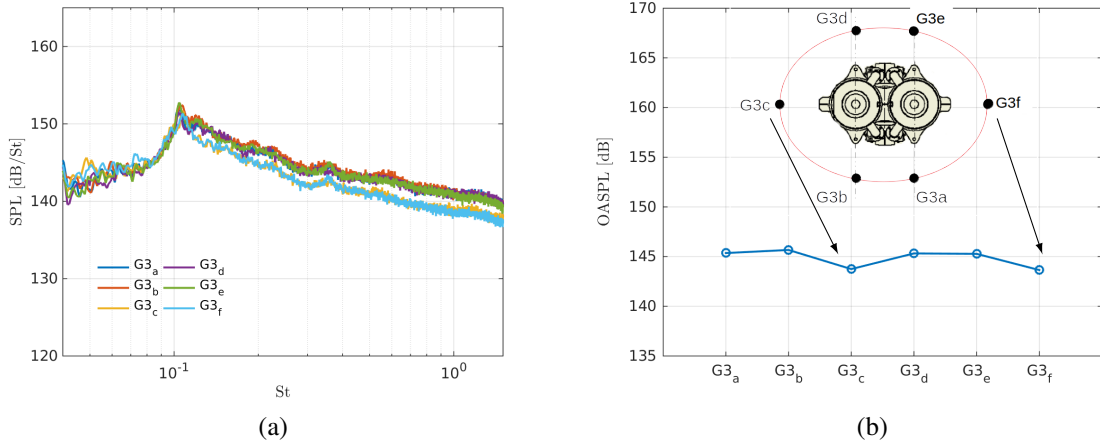


Figure 10: SPL and OASPL calculated on the oval antenna in the vicinity of the nozzle exit for the twin-jets configuration.

noise sources.

To quantitatively evaluate the acoustic field modifications induced by the jets proximity, we compare the results obtained with those relative to the single jet configuration. Figures 11c and 11d, show the noise intensity measured by the polar antennae AZ_b and AZ_c for the two azimuthal directions of interest. In the figures, the black dotted line corresponds the single-jet noise level plus 3 dB, which represents the total noise that would be obtained from a superposition of two identical jets with the hypothesis that no interaction occurs between the two. Interestingly, in the direction perpendicular to the plane containing the jet axis ($\phi = 90^\circ$), the measured noise nearly exactly correspond to a perfect superposition of independent jets, for all the polar angles. The source radiation in this direction is thus not affected by the presence of the second jet. On the other hand, for the observer positioned at $\phi = 0^\circ$, the noise increase for the twin-jets configuration is reduced to half (~ 1.5 dB). As already observed for the ring microphone near the nozzle exit, the noise sources radiating in that direction seem to be masked by the second jet.

In figures 11e and 11f, a spectral analysis of the jets interaction is presented. The two images, corresponding to the two azimuthal directions $\phi = 0^\circ$ and $\phi = 90^\circ$, show, as function of the Strouhal number St and the observation polar angle θ , the 'double-jet effect, defined as:

$$\Delta SPL = SPL_{twin-jets} - (SPL_{simple jet} + 3dB) \quad (1)$$

Following this definition, the white color in the images (value 0) corresponds to a measured noise, for the twin-jets configuration, equal to the exact superposition of two independent jets. The blue color indicates a beneficial interaction effect that causes a decrease of the emitted noise, while the red denotes an increased sound radiation. We observe that in the $\phi = 0^\circ$ direction, the measured noise reduction is almost constant for all the frequencies and at all the polar angles, with only a red spot near $\theta = 90^\circ$. On the other hand, a behaviour strongly dependent on the frequency is observed in the perpendicular plane ($\phi = 90^\circ$). A marked increase of the sound radiation is generated by the jets interaction for the lowest polar angles ($\theta \leq 60^\circ$) and in a frequency range of $0.07 \leq st \leq 0.3$. As the noise production at these angles is mainly associated with

the mixing mechanism, a possible explanation for the observed phenomenology can be related to a slight modification of the turbulent structures as the jets begin to merge.

5. CONCLUSIONS

An extensive experimental analysis of a twin, supersonic, heated jets configuration has been carried out in this work. Mean velocity measurements showed a very limited aerodynamic interaction between the two jets, for the geometric characteristics considered. On the other hand, a strongly asymmetric behaviour has been observed on the polar antennae in the acoustic field: a masking effect in the plane containing the jets axis causes a beneficial decrease of the radiated sound, constant for all the polar angles and a broad range of frequencies. In the perpendicular direction a marked increase of noise intensity appears in the lowest frequencies and polar angles, probably due to a turbulence field modification as the jets merge.

6. ACKNOWLEDGEMENTS

This work has been carried out in collaboration with the CNES (Centre Nationale d'Études Spaciales). The authors would like to specially thank Hadrien Lambaré.

7. REFERENCES

- [1] F. B. Greatrex and D. M. Brown. Progress in jet engine noise reduction. In *First Congress International Council of the Aeronautical Sciences*, 1958.
- [2] S Elangovan, A Solaiappan, and Ethirajan Rathakrishnan. Studies on twin non-parallel unventilated high-speed jets. *Proceedings of The Institution of Mechanical Engineers Part G-journal of Aerospace Engineering - PROC INST MECH ENG G-J A E*, 211:337–353, 05 1997.
- [3] M. B. Alkislar, A. Krothapalli, I. Choutapalli, and L. Lourenco. Structure of supersonic twin jets. *AIAA Journal*, 43, 2005.
- [4] Praveen Panickar, K Srinivasan, and Ganesh Raman. Aeroacoustic features of coupled twin jets with spanwise oblique shock-cells. *Journal of Sound and Vibration*, 278(1):155 – 179, 2004.
- [5] G. Raman, P. Panickar, and K. Chelliah. Aeroacoustics of twin supersonic jets: A review. *International Journal of Aeroacoustics*, 2012.
- [6] J.C Yu and D.J Fratello. Measurement of acoustic shielding by a turbulent jet. *Journal of Sound and Vibration*, 98(2):183 – 212, 1985.
- [7] P.Surendiren Parthasarathy, R F. Cuffel, and P F. Massier. Twin-jet shielding. *Journal of Aircraft*, 17, 04 1979.
- [8] C.K.W. Tam and H.K. Tanna. Shock associated noise of supersonic jets from convergent-divergent nozzles. *Journal of Sound and Vibration*, 81(3):337 – 358, 1982.

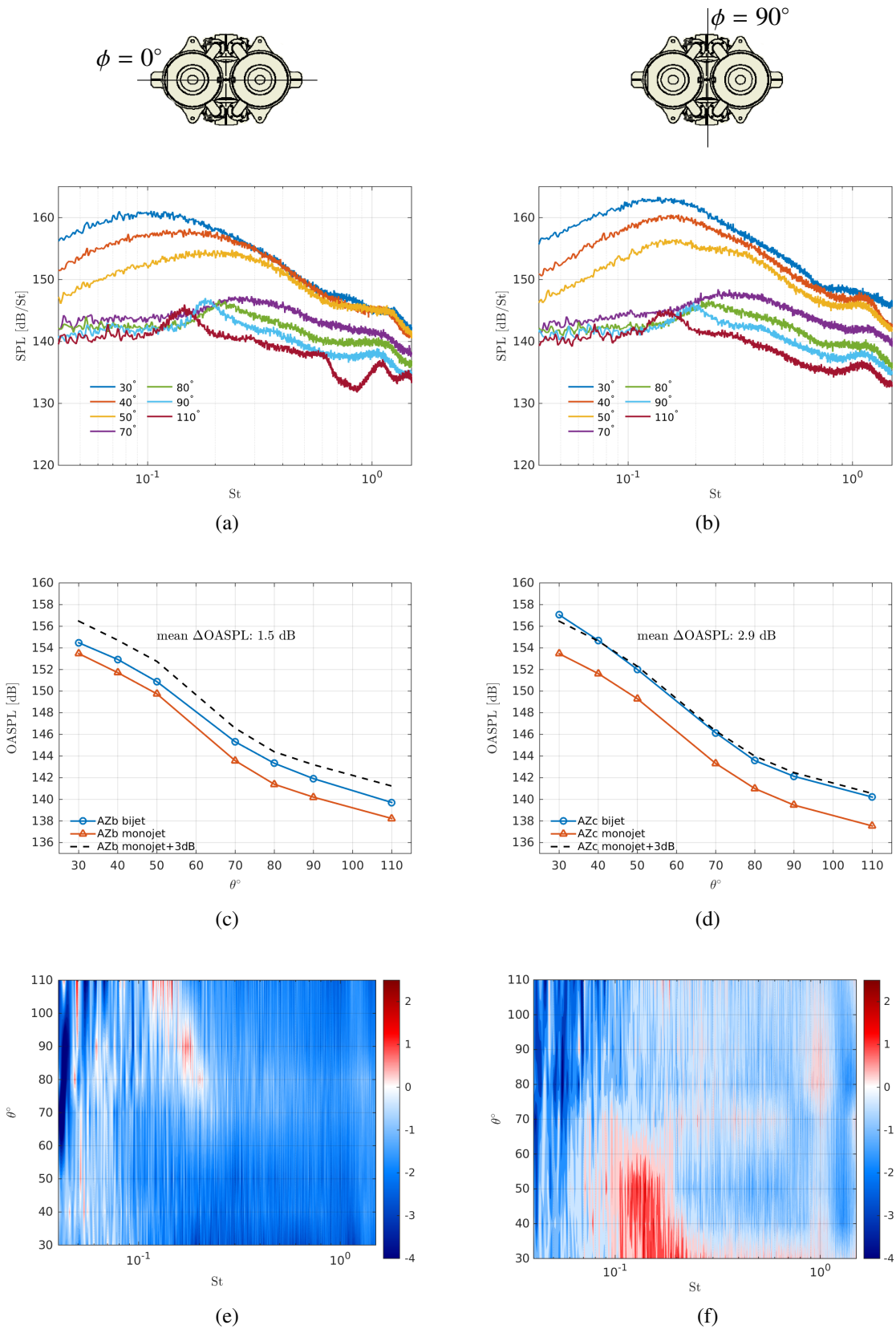


Figure 11: Polar SPL and OASPL calculated in the acoustic field for the twin-jets configuration.